

Platelet-rich Plasma Enhances Recovery of Skeletal Muscle Atrophy after Immobilization Stress in Rat: A Histological and Immunohistochemical Study

Heba H. Elkaliny, Shereen S. El-Abd and Marwa A. A. Ibrahim

Department of Histology and Cell Biology, Faculty of Medicine, Tanta University, Egypt

ABSTRACT

Background: Immobilization stress occurs in various clinical situations leading to disuse muscle atrophy. Recovery of skeletal muscle after immobilization is slow and incomplete. Platelet-rich plasma (PRP) was previously used in improving traumatic muscle injuries, yet, its role in accelerating muscle recovery upon immobilization stress has not been studied.

Aim of the Work: To study the possible adjuvant effect of PRP on skeletal muscle atrophy during recovery after immobilization stress in rat.

Material and Methods: Thirty-six adult male rats were equally divided into four groups; control, immobilization stress (restrained in reduced sized cages for 4 weeks), recovery alone (4 weeks), and recovery & PRP groups. Skeletal muscle specimens were processed for histological and immunohistochemical studies.

Results: Immobilized group showed splitting of the muscle fibers, internalization of the nuclei, loss of striation, undulated disrupted sarcolemma with signs of inflammation. Ultrastructural examination revealed myocytes with indented nuclei, mitochondria of abnormal shape and size, atrophied myofibrils with loss of myofilaments and splitting of myofibrils. A significant reduction of both mean muscle fiber cross sectional area and area percentage was reported together with a significant downregulation in desmin immunohistochemical expression. Recovery group revealed persistence of histological and immunohistochemical alterations. Recovery & PRP group showed a near normal morphology together with a non-significant difference in desmin immunohistochemical expression compared to control.

Conclusion: PRP offered a promising improvement of skeletal muscle atrophy after immobilization stress. It is recommended to apply adjuvant PRP therapy with recovery rather than recovery alone.

Received: 07 October 2020, **Accepted:** 30 October 2020

Key Words: Desmin; immobilization stress; PRP; recovery; skeletal muscle.

Corresponding Author: Marwa A. A. Ibrahim, MD, Department of Histology and Cell Biology, Faculty of Medicine, Tanta University, Egypt, Tel.: +20 1099186399, E-mail: rmarwa.ibrahim@med.tanta.edu.eg; maleox68@yahoo.com

ISSN: 1110-0559, Vol. 44, No.3

INTRODUCTION

Immobilization stress occurs in various clinical situations as chronic inflammatory and neuromuscular diseases, or it can even naturally occur in the elderly population. It eventually results in muscle disuse atrophy, which leads to limitations of daily activities and poor life quality. Moreover, in severe illness, extensive muscle atrophy increases morbidity and mortality of patients^[1].

Skeletal muscle is not only responsible for rapid, forceful, voluntary contraction, but it also carries out other functions including energy and protein metabolism, glucose uptake and storage, and acts as a storage site for amino acids in the form of protein, which is the body natural defense against nutritional, infectious or traumatic stress^[2,3]. Therefore, in case of muscular inactivity, the enhanced synthesis of reactive oxygen species (ROS) results in a decreased protein synthesis and muscle proteolysis, thus leading to a great damage of the muscle tissue structure and function, in addition to making the muscle more liable to hormonal catabolic signals than other muscles^[1,4].

Recovery of skeletal muscle after immobilization was argued to be slow, deficient and incomplete regardless of

its intrinsic capacity for recovery after atrophy^[5]. Previous studies suggested the role of physical exercising following a period of immobilization, yet, it is not always enough to restore the full muscle capacity^[4]. Therefore increasing muscle protein synthesis and/or decreasing muscle protein breakdown is an important adjuvant therapy for disuse atrophy. Many investigators proposed antioxidants as resveratrol^[6], mitochondrial antioxidant (SS-31)^[7] and vitamin E.^[8] Different treatment approaches as low intensity microcurrent therapy^[9], heat treatment^[10], and stem cell-based therapy^[11] were also suggested without reaching a resolute strategy.

Platelet-rich plasma (PRP) is that portion of blood with an above baseline platelet concentration. It has received a great interest in applied medicine as it can accelerate tissue healing and regeneration. Its role in curing traumatic muscle injuries through improving muscle regeneration, increasing neovascularization and reducing fibrosis was previously documented^[12,13], yet, its role in accelerating recovery of skeletal muscle atrophy after immobilization stress has not been studied.

Taken together, this work aimed to study the possible adjuvant effect of PRP on skeletal muscle atrophy during recovery after immobilization stress using different histological and immunohistochemical techniques.

MATERIAL AND METHODS

Experimental design

Thirty-six adult male albino rats, weighing 180-200 grams each, were used in this experiment. The rats had free access to balanced laboratory diet and water. The rats were acclimatized for 2 weeks before the experiment at the animal house. The study was approved by the Research Ethics Committee of Tanta Faculty of Medicine, Egypt.

The rats were allocated into four groups in a random manner:

Group I (Control group) n=9: Animals of this group were kept in standard sized cages (dimensions; 42 x 21 x 20 cm), they were further subdivided into 3 equal subgroups; Animals of subgroup Ia were kept for 4 weeks without any treatment. Animals of subgroup Ib received a single intramuscular injection with 0.5 ml of saline in the right gastrocnemius muscle then kept for 4 weeks. Animals of subgroup Ic received 0.5 ml of PRP as a single intramuscular injection in the right gastrocnemius muscle then were kept for 4 weeks without further treatment.

Group II (Immobilization stress group) n=9: Animals of this group were restrained in reduced size cages (dimensions; 12 x 12 x 8 cm) for 4 weeks^[14].

Group III (Immobilization stress recovery group) n=9: Animals of this group were kept in reduced size cages for 4 weeks then transferred to standard sized cages for another 4 weeks.

Group IV (Immobilization stress recovery & PRP group) n=9: Animals of this group were kept in reduced size cages for 4 weeks then 0.5 ml of PRP as a single intramuscular injection in the right gastrocnemius muscle before being transferred to standard sized cages for another 4 weeks.

PRP was prepared according to Ariede *et al.*^[15] where blood samples were collected from rats in citrated vials under anesthesia. The whole blood underwent centrifugation (3000 rpm, 7 min, 20°C) to sediment down red blood cells. The plasma supernatant was aspirated and further centrifuged (4000 rpm, 5 min, 20°C) to collect down the platelet-rich plasma fraction for intramuscular injection.

The animals were eventually euthanized using pentobarbital (40 mg/kg)^[16]. The right gastrocnemius muscle was rapidly dissected out to be processed for light and transmission electron microscopy.

Histological preparation for light microscopy

Skeletal muscle specimens were fixed using 10% neutral buffered formalin, washed, dehydrated, cleared,

and paraffinized. Sections of 5 µm thickness were stained with hematoxylin & eosin (H&E)^[17].

Immunohistochemical staining

Sections were deparaffinized, rehydrated and washed then incubated with 10% normal goat serum in phosphate buffered saline. Sections were incubated with the primary antibody; rabbit polyclonal antibody against desmin (ab15200, Abcam, Cambridge, Massachusetts, USA) overnight at 4°C, then incubated with the secondary antibody for 60 min at room temperature then with a streptavidin–biotin–horseradish peroxidase complex for another 60 min. 3,3'-diaminobenzidine (DAB) hydrogen peroxide was used to visualize the immunoreactivity. Counterstaining was applied using Mayer's hematoxylin^[18].

Histological preparation for transmission electron microscopy

Skeletal muscle specimens were finely cut and fixed using 4% phosphate buffered glutaraldehyde then post-fixed using 1% phosphate-buffered osmium tetroxide then dehydrated. Propylene oxide was used to immerse the specimens then epoxy resin mixture was used for embedding them. Staining with uranyl acetate and lead citrate was applied for the ultrathin sections (80-90nm)^[19] to be examined using JEOL-JEM-100 transmission electron microscope (Tokyo, Japan) at the Electron Microscopy Unit, Tanta Faculty of Medicine, Egypt.

Morphometric analysis

A light microscope (Leica DM500, Switzerland) connected to a digital camera (Leica ICC50, Switzerland) was used to obtain images. The software "ImageJ" (1.48 NIH, USA) was used for image analysis. Ten different non-overlapping randomly selected fields from each slide were examined at a magnification of 400 to quantitatively evaluate:

1. Mean muscle fiber cross sectional area (µm²) and area percentage (%) (in H&E-stained sections).
2. Mean optical density of desmin immunohistochemical reaction (in DAB-stained sections)^[20].

Statistical analysis

The data were analyzed by using ANOVA followed by Tukey's test using IBM SPSS Statistics for Windows (IBM Corp, Version 22.0. Armonk, NY, USA). Differences were considered as significant if probability value $p < 0.05$ and highly significant if $p < 0.001$ ^[21].

RESULTS

H&E staining

Control group

The gastrocnemius muscle from rats of all control subgroups showed the normal structure of skeletal muscle formed of muscle bundles separated by perimysium

connective tissue. In longitudinal sections, the muscle fibers were parallel, elongated, cylindrical and non-branched with acidophilic cytoplasm, regular striations and multiple flat nuclei underneath the sarcolemma (Figure 1a). In cross sections, polyhedral muscle fibers with oval peripheral nuclei were observed, where each muscle fiber was enclosed by loose endomysium connective tissue (Figure 1b).

Immobilization stress group

Longitudinal sections from immobilization stress group showed splitting and branching of the muscle fibers with internalization of the nuclei. Some muscle fibers showed loss of striation and undulated disrupted sarcolemma. Other muscle fibers exhibited multiple lightly stained foci. Some dilated congested blood vessels and mononuclear cell infiltration were observed. Separation of endomysium with connective tissue cells and blood capillaries was detected (Figures 2,3).

Cross sections showed muscle fibers of variable size and shape. Muscle fibers were mostly fragmented with separation of endomysium containing connective tissue cells and blood capillaries with exudate. Some muscle fibers were apparently shrunken. Multiple lightly stained foci of muscle fibers were observed. Some muscle fibers showed centralization of some nuclei (Figures 4,5).

Recovery group

Longitudinal sections from recovery group showed few muscle fibers with splitting, sarcolemmal disruption and internalization of the nuclei. Few areas of absent striation and lightly stained foci were observed. Mononuclear cell infiltration was also encountered (Figure 6). Moreover, cross sections revealed some fragmented muscle fibers with separation of endomysium and mononuclear cell infiltration. Few muscle fibers were apparently shrunken among the apparently normal muscle fibers (Figure 7).

Recovery and PRP group

Longitudinal sections from recovery and PRP group depicted apparently normal skeletal muscle fibers with regular striations and multiple flat nuclei (Figure 8). Cross sections revealed apparently normal polyhedral muscle fibers with oval peripheral nuclei (Figure 9).

Morphometrical analysis of the mean muscle fiber cross sectional area and area percentage in group II (1100.22 ± 75.7 , 68.69 ± 6.04 respectively) revealed a highly significant decrease compared to control (1881.22 ± 96.11 , 81.22 ± 6.21 respectively), while group III (1666.09 ± 90.31 , 75.05 ± 6.77 respectively) showed a significant increase compared to group II, yet it represented a significant decrease compared to control. Instead, group IV (1820.98 ± 94.76 , 79.41 ± 7.98 respectively) depicted a significant increase compared to both groups II and III, which represented a non-significant difference from the control (Table 1, Histogram 1).

Desmin immunohistochemical staining

Immunohistochemically stained muscle sections for detection of desmin in control group depicted a strong subsarcolemmal and sarcoplasmic desmin expression in the form of a brownish coloration (Figure 10). Whereas sections from immobilization stress group II revealed a weak desmin expression (Figure 11). Whereas sections from recovery group III depicted a moderate desmin expression (Figure 12). Nevertheless, sections from recovery & PRP group IV showed a strong desmin expression (Figure 13).

Morphometrical analysis of the optical density of desmin immunoexpression in group II (37.90 ± 8.63) showed a highly significant decline with comparison to the control (67.83 ± 5.99), while group III (59.94 ± 7.06) revealed a significant elevation compared to group II, which still represented a significant decline compared to the control. Conversely, group IV (65.94 ± 3.96) depicted a significant elevation compared to both groups II and III, which represented a non-significant difference from the control (Table 1, Histogram 1).

Transmission Electron Microscopy

Control group

Ultrastructural examination of control group showed myocytes with longitudinal myofibrils and flattened peripheral euchromatic nucleus underneath the sarcolemma with prominent nucleolus. The muscle fibrils depicted alternating dark (A) and light (I) bands. The dark (Z) line bisected the light (I) band, the dark (A) band was bisected by a narrow lighter (H) zone that was further halved by a dark (M) line. Small mitochondria were paired around the Z lines and some larger ones were perinuclear (Figure 14).

Immobilization stress group

Ultrastructural examination of immobilization stress group revealed myocytes with indented nuclei, focal distortion of the (Z) lines in some myofibrils and mitochondria of abnormal shape and size. Some myocytes depicted giant amorphous mitochondria. Areas of atrophied myofibrils with loss of myofilaments and splitting of some myofibrils were detected (Figures 15-18).

Recovery group

Ultrastructural examination of recovery group depicted myocytes with peripheral euchromatic nucleus and prominent nucleolus. Few areas of myofibrillar loss were detected. Giant mitochondria were frequently observed around the nuclei and Z lines (Figure 19).

Recovery and PRP group

Ultrastructural examination of recovery & PRP group showed apparently normal myocytes with peripheral euchromatic nuclei, intact longitudinal myofibrils and apparently normal mitochondria (Figures 20, 21).

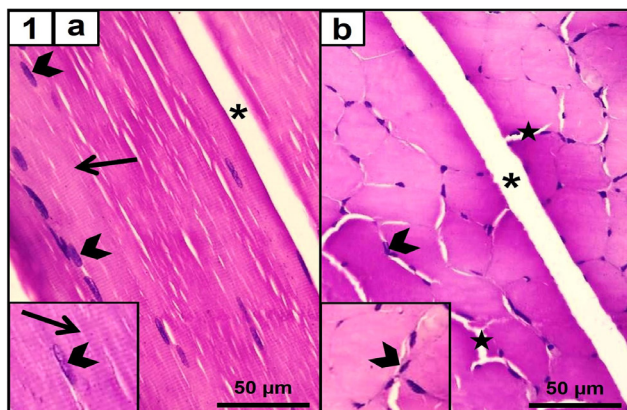


Fig. 1: A photomicrograph of the gastrocnemius muscle from control rat shows muscle bundles separated by perimysium connective tissue (asterisks). a) Longitudinal sections show parallel, elongated, cylindrical and non-branched muscle fibers with regular striations (thin arrows) and multiple flat nuclei underneath the sarcolemma (arrowheads). b) Cross sections show polyhedral muscle fibers with oval peripheral nuclei (arrowheads), each muscle fiber is enclosed by loose endomysium CT (stars). (H&E x 400, scale bar=50 µm, inset x 1000).

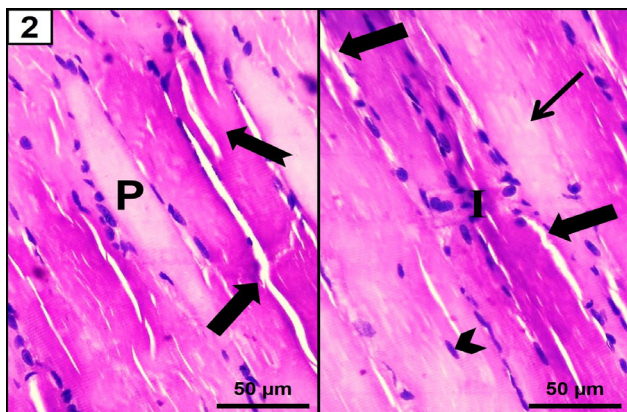


Fig. 2: A photomicrograph of a longitudinal section in the gastrocnemius muscle from immobilization group shows splitting and branching of the muscle fibers (notched arrow) and internalization of the nuclei (arrowhead). Some muscle fibers show loss of striation (thin arrow) and undulated disrupted sarcolemma (thick arrows). Other muscle fibers exhibit lightly stained foci (P) and mononuclear cell infiltration (I) (H&E x400, scale bar=50 µm)

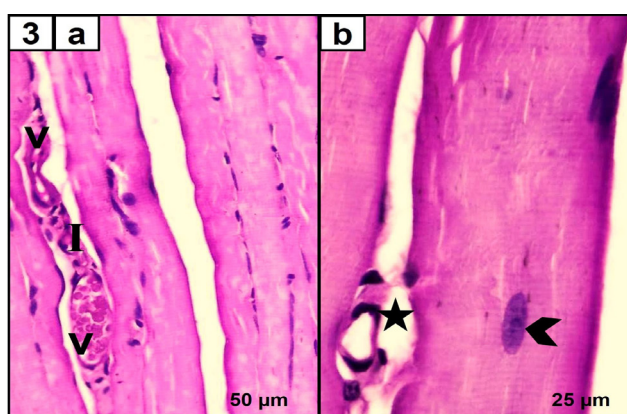


Fig. 3: A photomicrograph of a longitudinal section in the gastrocnemius muscle from immobilization group shows some dilated congested blood vessels (V) associating with mononuclear cell infiltration (I). Separation of endomysium (star), with connective tissue cells and blood capillaries, and internalization of some nuclei (arrowhead) are detected (H&E x400, b x1000)

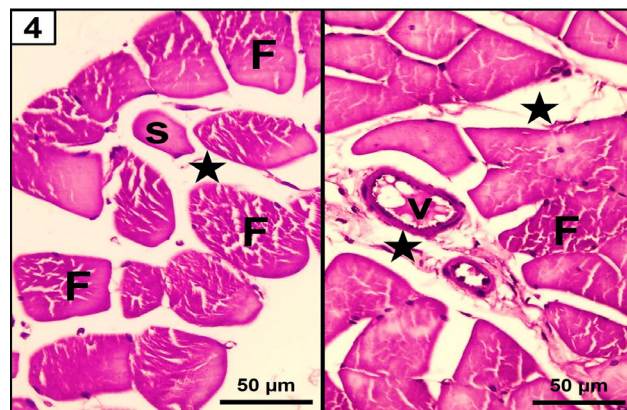


Fig. 4: A photomicrograph of a cross section in the gastrocnemius muscle from immobilization group shows muscle fibers of variable size and shape. Most of the muscle fibers are fragmented (F) with separation of endomysium (stars) containing connective tissue cells and blood capillaries (v) with exudate. Some muscle fibers are apparently shrunken (s). (H&E x400, scale bar=50 µm)

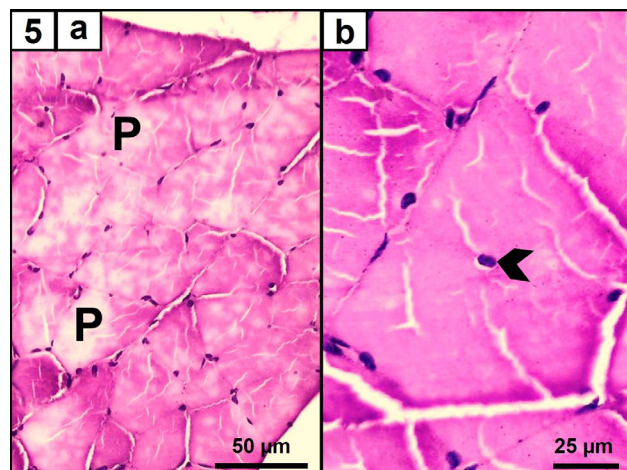


Fig. 5: A photomicrograph of a cross section in the gastrocnemius muscle from immobilization group shows multiple lightly stained foci of muscle fibers (P). Some muscle fibers show centralization of some nuclei (arrowhead) (H&E, a x400, b x1000)

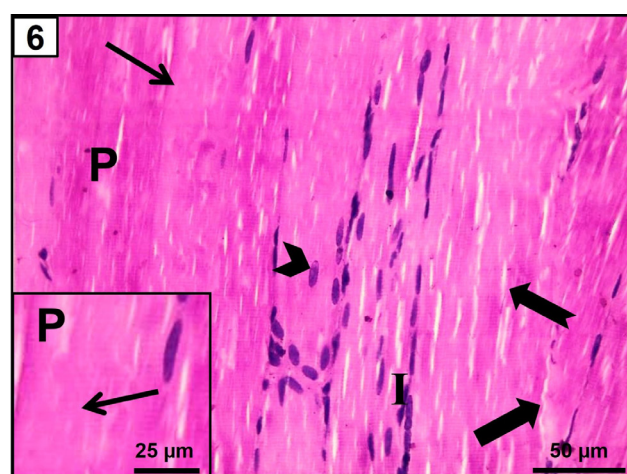


Fig. 6: A photomicrograph of a longitudinal section in the gastrocnemius muscle from recovery group shows few muscle fibers with splitting (notched arrow), sarcolemmal disruption (thick arrow) and internalization of the nuclei (arrowhead). Few areas of absent striation (thin arrow) and lightly stained foci (P) are observed. Mononuclear cell infiltration (I) is detected. (H&E x400, scale bar=50 µm)

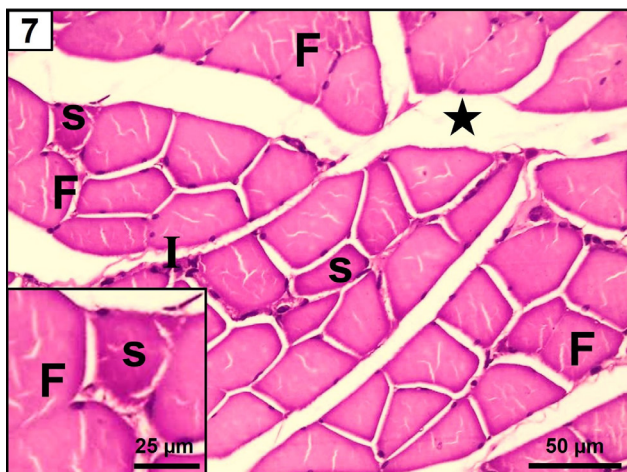


Fig. 7: A photomicrograph of a cross section in the gastrocnemius muscle from recovery group shows some fragmented muscle fibers (F) with separation of endomysium (star) and mononuclear cell infiltration (I). Few muscle fibers are apparently shrunken (s) among the apparently normal muscle fibers. (H&E x400, scale bar=50 μ m, inset x 1000)

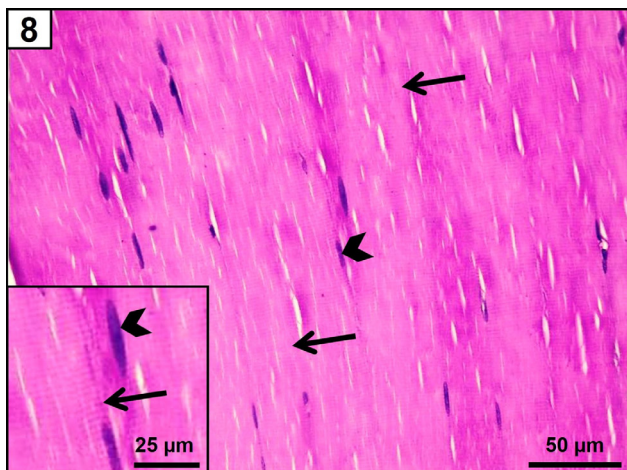


Fig. 8: A photomicrograph of a longitudinal section in the gastrocnemius muscle from recovery & PRP group shows apparently normal skeletal muscle fibers with regular striations (thin arrows) and multiple flat nuclei (arrowhead). (H&E x400, scale bar=50 μ m, inset x 1000)

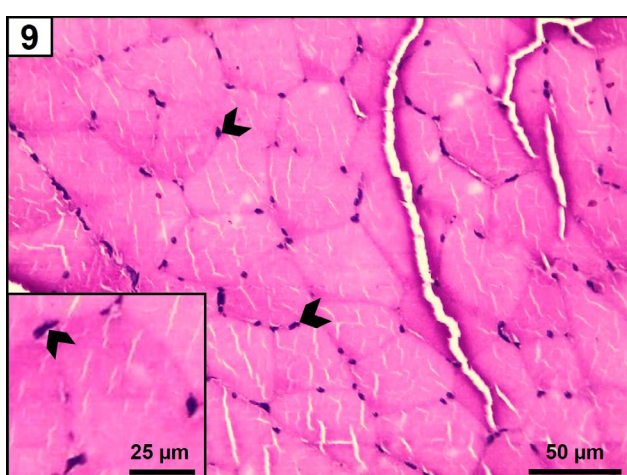


Fig. 9: A photomicrograph of a cross section in the gastrocnemius muscle from recovery & PRP group shows apparently normal polyhedral muscle fibers with oval peripheral nuclei (arrow heads) (H&E x400, scale bar=50 μ m, inset x 1000)

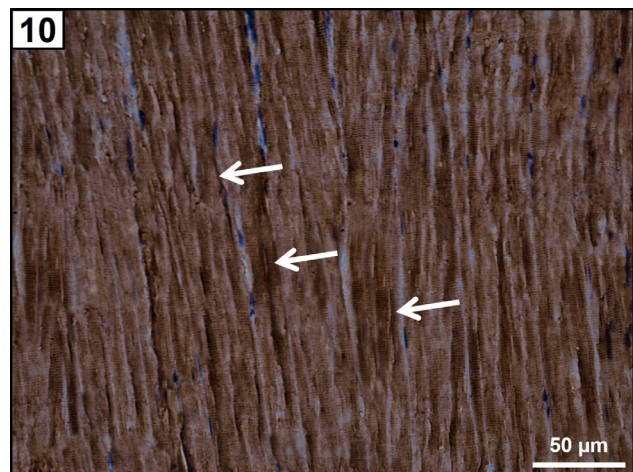


Fig. 10: A photomicrograph of the gastrocnemius muscle from control group shows a strong subsarcolemmal and sarcoplasmic desmin expression in the form of a brownish coloration (arrows) (Desmin x 400, scale bar=50 μ m)

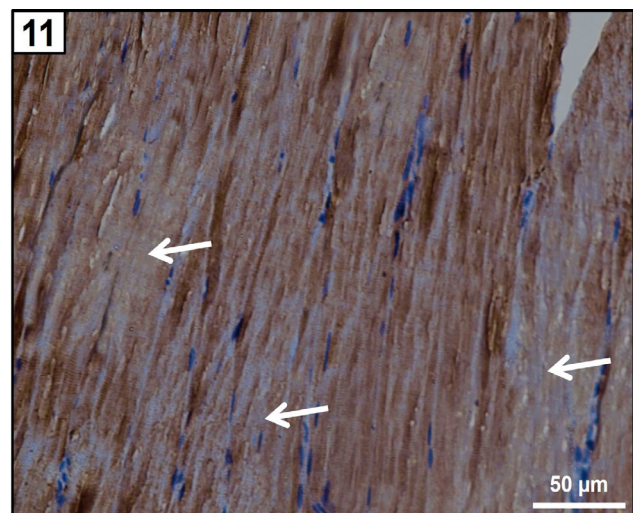


Fig. 11: A photomicrograph of the gastrocnemius muscle from immobilization group showing a weak sarcoplasmic desmin expression (arrows) (Desmin x 400, scale bar=50 μ m)



Fig. 12: A photomicrograph of the gastrocnemius muscle from recovery group shows a moderate subsarcolemmal and sarcoplasmic desmin expression (arrows) (Desmin x 400, scale bar=50 μ m)

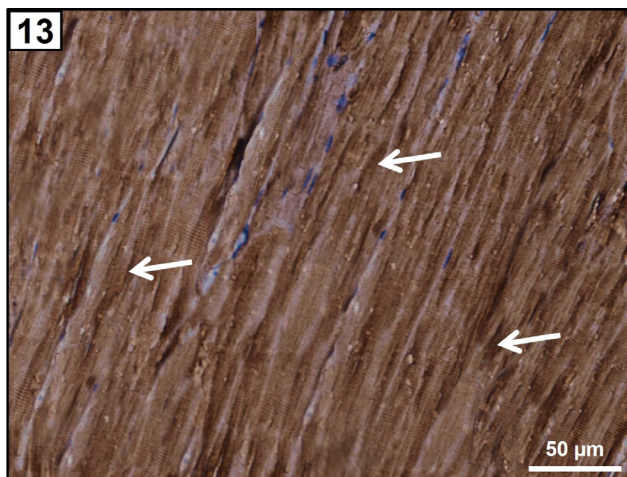


Fig. 13: A photomicrograph of the gastrocnemius muscle from recovery & PRP group shows a strong subsarcolemmal and sarcoplasmic desmin expression (arrows) (Desmin x 400, scale bar=50 μ m)

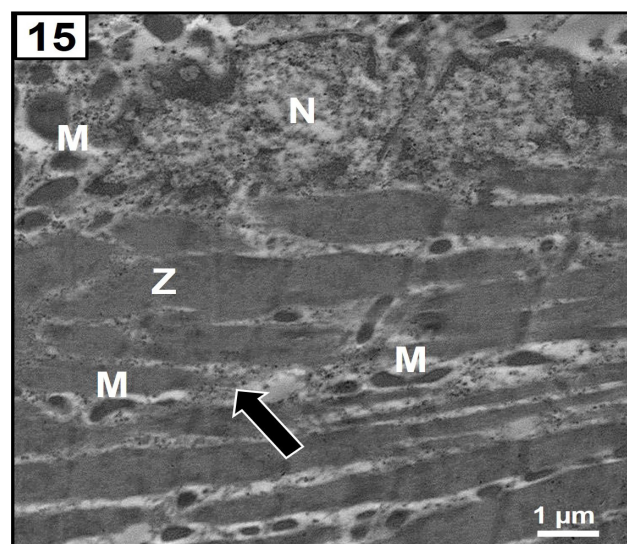


Fig. 15: An electron photomicrograph from immobilization group shows a myocyte with an indented nucleus (N). Areas of myofibrillar loss (thick arrow) and focal distortion of the (Z) lines in some myofibrils are observed. Notice mitochondria are of bizarre shape and size (M). (TEM x17500, scale bar=1 micron)

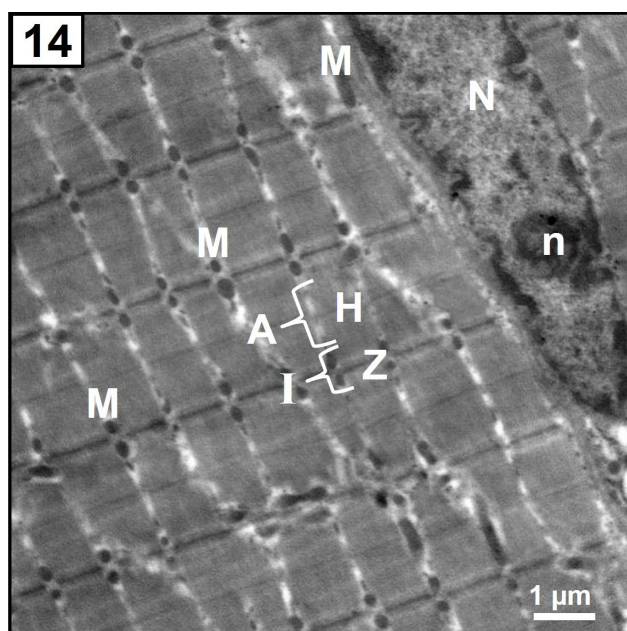


Fig. 14: An electron photomicrograph from control group shows a myocyte with longitudinal myofibrils and flattened peripheral euchromatic nucleus (N) just beneath the sarcolemma with prominent nucleolus (n). The muscle fibrils show alternating dark (A) and light (I) bands. The dark (Z) line bisects the light (I) band, the dark (A) band is bisected by a narrow lighter (H) zone that is further halved by a dark (M) line. Small mitochondria (M) are paired around the Z lines and some larger ones are perinuclear. (TEMx 17500, scale bar=1 micron)

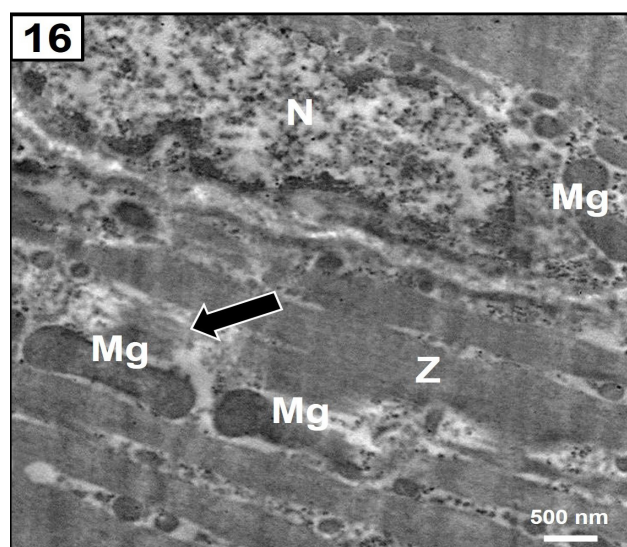


Fig. 16: An electron photomicrograph from immobilization group shows a myocyte with an indented nucleus (N). Areas of myofibrillar loss (thick arrow) and focal distortion of the (Z) lines in some myofibrils are observed. Notice giant amorphous mitochondria (Mg). (TEM x29200, scale bar=500nm)

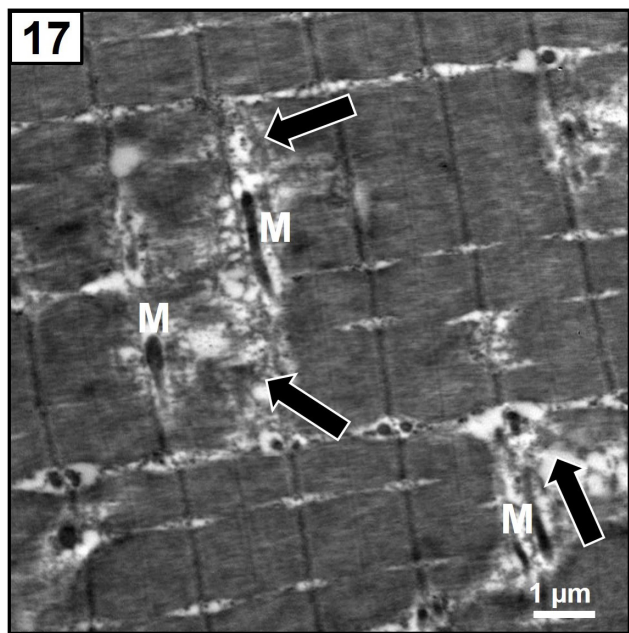


Fig. 17: An electron photomicrograph from immobilization group shows areas of atrophied myofibrils and loss of myofilaments (thick arrows) with bizarre shaped mitochondria (M). (TEM x17500, scale bar=1 micron)

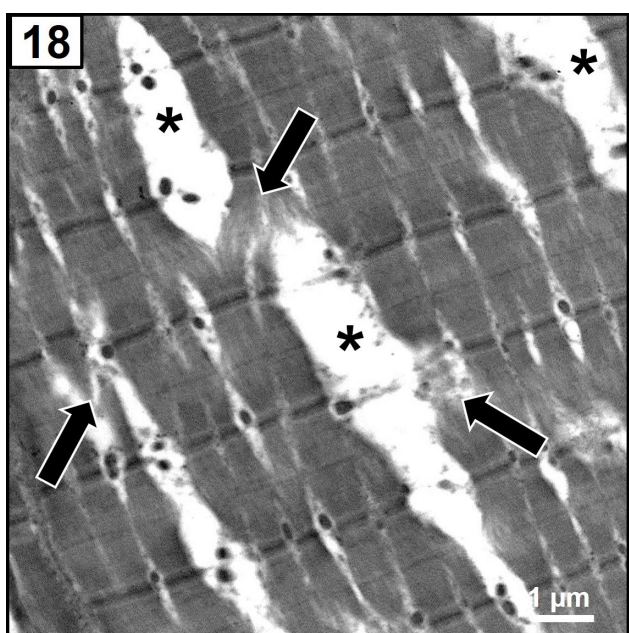


Fig. 18: An electron photomicrograph from immobilization group showing areas of atrophied myofibrils and loss of myofilaments (thick arrows). Notice splitting of some myofibrils (asterisks). (TEM x17500, scale bar=1 micron)

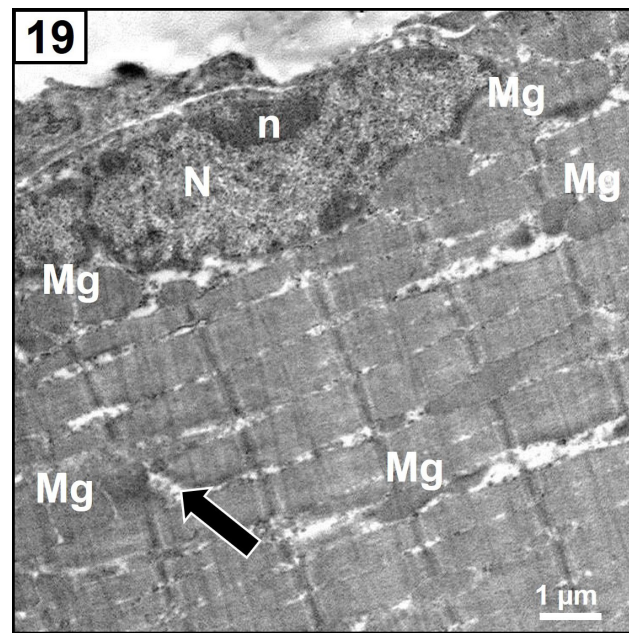


Fig. 19: An electron photomicrograph from recovery group shows a myocyte with peripheral euchromatic nucleus (N) with prominent nucleolus (n). Few areas of myofibrillar loss (thick arrow) are detected. Giant mitochondria (Mg) are observed around the nuclei and Z lines. (TEM x17500, scale bar=1 micron)

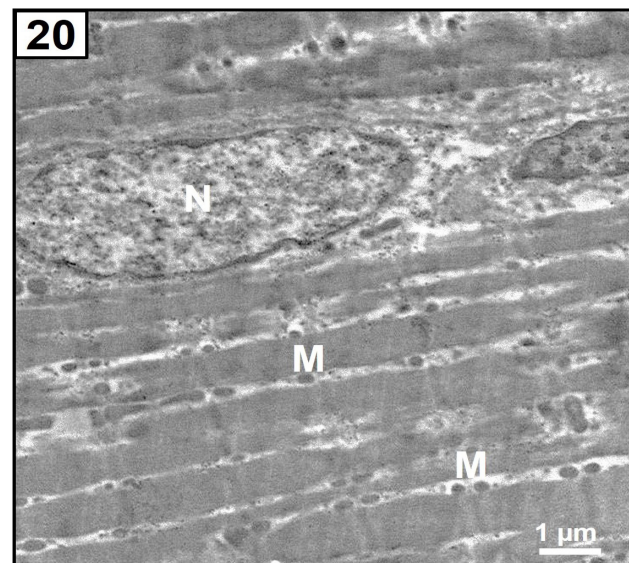


Fig. 20: An electron photomicrograph from recovery & PRP group shows an apparently normal myocyte with peripheral euchromatic nucleus (N), several intact longitudinal myofibrils and apparently normal mitochondria (M). (TEM x17500, scale bar=1 micron)

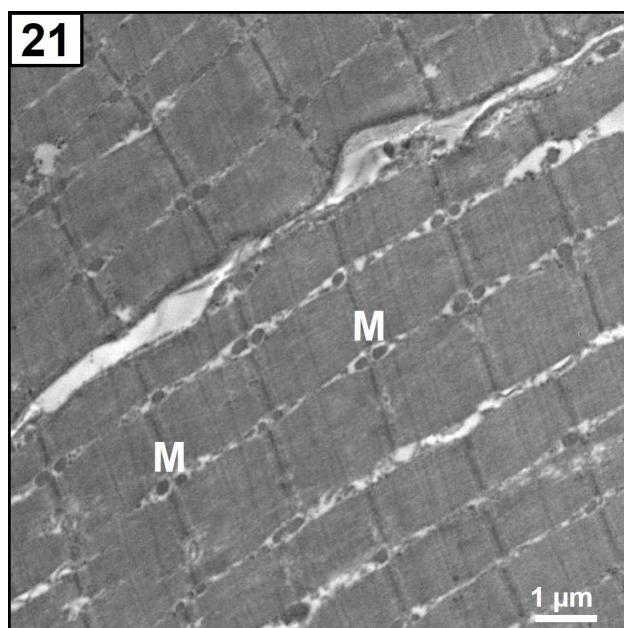
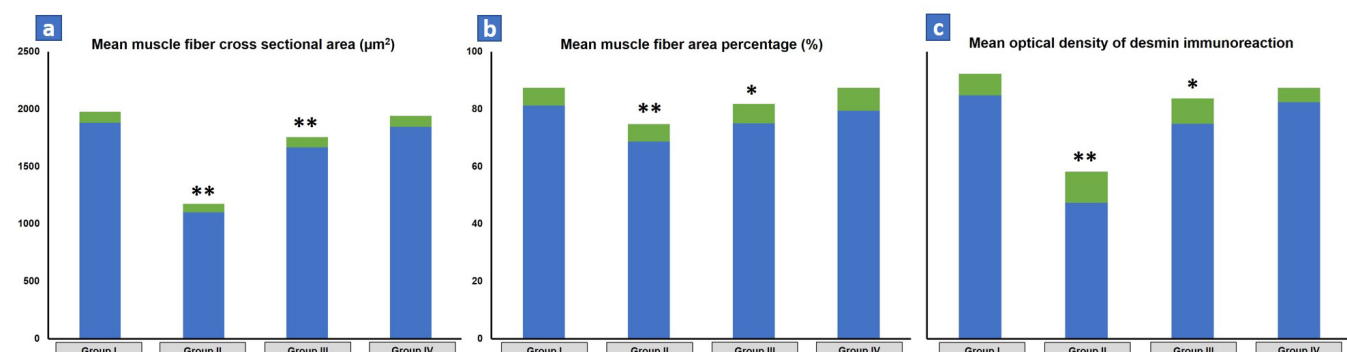


Fig. 21: An electron photomicrograph from recovery & PRP group shows an apparently normal myocyte with several intact longitudinal myofibrils and apparently normal mitochondria (M). (TEM x17500, scale bar=1 micron)

Table 1: Statistical analysis of the study groups

Parameters	Group I	Group II	Group III	Group IV
Mean muscle fiber cross sectional area (μm^2)	1881.22 \pm 96.11	1100.22 \pm 75.7**	1666.09 \pm 90.31**	1820.98 \pm 94.76
Mean muscle fiber area percentage (%)	81.22 \pm 6.21	68.69 \pm 6.04**	75.05 \pm 6.77*	79.41 \pm 7.98
Mean optical density of desmin immunoreaction	67.83 \pm 5.99	37.90 \pm 8.63**	59.94 \pm 7.06*	65.94 \pm 3.96

Data is expressed as mean \pm standard deviation. * indicates significant vs control, ** indicates highly significant vs control



Histogram 1: Morphometrical analysis of a] Mean muscle fiber cross sectional area (μm^2), b] Mean muscle fiber area percentage (%), c] Mean optical density of desmin immunoreaction. * indicates significant vs control, ** indicates highly significant vs control

DISCUSSION

Immobilization is used in clinical practice during the treatment of many serious diseases, pain reduction and healing fractures. Brief periods of immobilization equally impose serious risks, especially muscle atrophy, as prolonged ones^[4,22]. In the current research, a physiological model simulating prolonged bed stay in humans was used, where rats were immobilized by keeping them in reduced size cages for 4 weeks^[14].

In the current work, longitudinal muscle sections from the immobilization stress group revealed undulated

disrupted sarcolemma which could be attributed to an elevation in production of ROS causing lipid peroxidation, thus affecting cell membranes assembly and changing physicochemical properties and cellular metabolic processes causing cell death^[23].

Additionally, separation of endomysium with signs of inflammation were observed in the current work. This agreed with other researchers who observed that the interstitial tissue was interspersed with hemorrhagic foci accompanied with marked inflammatory cell infiltration^[24,25]. These findings might be attributed to the release of certain mediators which stimulate inflammatory

reaction and attract inflammatory cells to invade the muscle, contribute to mechanisms of degradation and play a crucial role in getting rid of necrotic fiber segments^[26].

Furthermore, there were splitting, branching and loss of striation with internalization of the nuclei during the present work, which agreed with many researchers who stated that splitting of muscle fibers with centralized nuclei and homogenous eosinophilic structureless bundles with complete loss of normal fibers striation are well known features of muscle atrophy^[24,27,28].

In the present study, cross muscle sections from the immobilization stress group revealed that most of the muscle fibers were fragmented while other muscle fibers were apparently shrunken. Also, some muscle fibers depicted centralization of some nuclei. These results coincided with the work of Dumitru *et al.*^[29] who stated that skeletal muscle atrophy had common histopathological features as reduction of myofibers diameter, fragmented myofibers, and myofibers with central nuclei. These histopathological findings upon muscle atrophy are caused by proteolytic systems, whose activation leads to degradation of the proteins responsible for contraction resulting in muscle fibers fragmentation, shrinkage and loss of striation^[30].

The myonuclear positioning is important for cell function, it is mediated by microtubules and cytoplasmic intermediate filaments. The centralization of nuclei is mostly caused by desmin intermediate filament, that is the main muscle-specific structural protein that was suggested to be in charge for intracellular mechanochemical signaling and transport, thus has a fundamental role in spacing of nuclei^[31]. During atrophy, desmin is degraded by proteolytic pathways leading to mispositioning of nuclei^[32,33], which was confirmed by the significant downregulation in desmin immunohistochemical expression in the immobilization stress group in the current study.

Moreover, a significant reduction of both mean muscle fiber cross sectional area and area percentage was recorded in the immobilization stress group compared to control. These findings coincided with other reports that indicated that the myofiber cross sectional area was reduced by around 34% in immobilized group compared to control, thus confirmed the atrophy of muscle fibers during muscle disuse^[34]. Furthermore, the mean fiber cross sectional area was reported to significantly drop in the muscle of middle-aged adults after 14 days of bed rest^[35].

In the current work, ultrastructural assessment of the immobilization stress group revealed areas of myofibrillar loss, atrophied myofibrils with loss of myofilaments and splitting of others in addition to focal distortion of the (Z) lines. These findings could explain the existence of lightly stained foci detected with light microscopy during the present study and coincided other previous reports^[36]. These results could be attributed to protein degradation through ubiquitin proteasomal and lysosomal systems^[37,38]. Additionally, other researchers reported that two ubiquitin ligases, atrogin-1/MAFbx and muscle RING-finger 1 were markedly induced during muscle atrophy^[39,40].

Another electron microscopic finding from the immobilization stress group of the present study was mitochondria of abnormal shape and size and even some giant amorphous mitochondria. This coincided with previous researches that reported changes in mitochondrial size and shape, swelling, cristae breaking, reduced density, and vacuolation of mitochondria^[36]. Mitochondria are highly dynamic, where their function and morphology are controlled by fusion and fission events, whereas during muscle atrophy, the structure and function of mitochondria undergo dramatic changes. Furthermore, the increased ROS in atrophied muscles was suggested to significantly provoke the transcription factors responsible for mitochondrial dysfunction^[41,42].

The most accepted mechanism of disuse atrophy is the drop in protein synthesis coupling with a boost in protein degradation, since the skeletal muscle mass is delicately balanced between protein synthesis and degradation. Extended periods of immobilization cause an increased production of ROS in the muscle fibers suggesting the fundamental role of ROS in the process of disuse atrophy as ROS can enhance proteolysis and suppress protein synthesis^[34,43]. Nevertheless, immobilization suppresses protein synthesis through downregulating signaling of insulin like growth factor 1 (Igf1), which is an important anabolic growth factor for regulating protein metabolism and muscle growth. Igf1 activates the phosphatidylinositol-3 kinase (PI3K)/Akt pathway which in turn activates mTOR enhancing protein synthesis^[44,45].

In the present work, examination of recovery group revealed persistence of muscle atrophy morphological alterations, while recovery & PRP group depicted a near control skeletal muscle structure. Furthermore, the mean muscle fiber cross sectional area, area percentage and desmin immunohistochemical expression of recovery & PRP group recorded a significant increase compared to both the immobilization stress and recovery group, while represented a non-significant difference from control, thus strongly suggesting the efficacy of PRP in alleviating disuse muscle atrophy and accelerating muscle regeneration. Many studies reported that PRP administration could improve morphology, function and decrease inflammatory state of damaged skeletal muscles^[46]. PRP is used to obtain many cytokines and growth factors which can be an adjunctive measure to help in tissue regeneration process. Many evidences supported that growth factors are extremely needed during the muscle regeneration processes^[47]. Platelets contain nearly more than 300 molecules as calcium ions, serotonin, adenosine diphosphate, and polyphosphates. These molecules play a crucial role in the activation of other platelets, whose granules are in turn degranulated to liberate many growth factors; insulin like growth factor (IGF-1, IGF-2), fibroblast growth factor (FGF), tumor growth factor (TGF-β), platelet-derived growth factor (PDGF), hepatocyte growth factor, matrix metalloproteinases, interleukin 8 and many other cytokines^[48,49].

IGF-1 is proposed to provoke differentiation and proliferation of myoblasts and enhance regeneration in mouse skeletal muscle^[50]. Also, FGF-2 proved efficient in promoting both number and diameter of regenerating muscle fibers, while TGF- β aids additional growth factors such as PDGF which is capable of provoking satellite cell activation^[51], leading to expression of different myogenic regulatory factors and modulation of the expression of muscle specific microRNAs, and consecutively improving the function of mitochondria and their endogenous antioxidant defense system and ultimately protecting cells from apoptosis[46].

CONCLUSION

PRP is a simple and minimally invasive method that offers a promising improvement of skeletal muscle atrophy after immobilization stress. It is recommended to apply adjuvant PRP therapy along with recovery rather than recovery alone.

CONFLICT OF INTERESTS

There are no conflicts of interest.

REFERENCES

- Powers SK, Lynch GS, Murphy KT, Reid MB, Zijdewind I. Disease-Induced Skeletal Muscle Atrophy and Fatigue. *Med Sci Sports Exerc* 2016;48:2307–19.
- Magne H, Savary-Auzeloux I, Vazeille E, et al. Lack of muscle recovery after immobilization in old rats does not result from a defect in normalization of the ubiquitin-proteasome and the caspase-dependent apoptotic pathways. *J Physiol* 2011;589:511–24.
- Argilés JM, Campos N, Lopez-Pedrosa JM, Rueda R, Rodriguez-Mañas L. Skeletal Muscle Regulates Metabolism via Interorgan Crosstalk: Roles in Health and Disease. *J Am Med Dir Assoc* 2016;17:789–96.
- Koike TE, Watanabe AY, Kodama FY, et al. Physical Exercise After Immobilization Of Skeletal Muscle Of Adult And Aged Rats. *Rev Bras Med do Esporte* 2018;24:60–3.
- Fujitani M, Mizushige T, Kawabata F, et al. Dietary Alaska pollack protein improves skeletal muscle weight recovery after immobilization-induced atrophy in rats. *PLoS One* 2019;14:e0217917–e0217917.
- Momken I, Stevens L, Bergouignan A, et al. Resveratrol prevents the wasting disorders of mechanical unloading by acting as a physical exercise mimetic in the rat. *FASEB J* 2011;25:3646–60.
- Talbert EE, Smuder AJ, Min K, Kwon OS, Szeto HH, Powers SK. Immobilization-induced activation of key proteolytic systems in skeletal muscles is prevented by a mitochondria-targeted antioxidant. *J Appl Physiol* 2013;115:529–38.
- Powers SK. Can antioxidants protect against disuse muscle atrophy? *Sports Med* 2014;44 Suppl 2:S155–65.
- Moon YS, Kwon DR, Lee Y. Therapeutic effect of microcurrent on calf muscle atrophy in immobilized rabbit. *Muscle Nerve* 2018;58:270–6.
- Hafen PS, Abbott K, Bowden J, Lopiano R, Hancock CR, Hyldahl RD. Daily heat treatment maintains mitochondrial function and attenuates atrophy in human skeletal muscle subjected to immobilization. *J Appl Physiol* 2019;127:47–57.
- Dunn A, Talovic M, Patel K, Patel A, Marcinczyk M, Garg K. Biomaterial and stem cell-based strategies for skeletal muscle regeneration. *J Orthop Res* 2019;37:1246–62.
- Wasterlain AS, Braun HJ, Harris AHS, Kim H-J, Dragoo JL. The Systemic Effects of Platelet-Rich Plasma Injection. *Am J Sports Med* 2012;41:186–93.
- Bubnov R. Ultrasound guided injections of Platelets Rich Plasma for muscle injury in professional athletes. Comparative study. *Med Ultrason* 2013;15:101–5.
- Marmonti E, Busquets S, Toledo M, et al. A Rat Immobilization Model Based on Cage Volume Reduction: A Physiological Model for Bed Rest? *Front Physiol* 2017;8:184.
- Ariede JR, Pardini MI de MC, Silva GF, Grotto RMT. Platelets can be a biological compartment for the Hepatitis C Virus. *Braz J Microbiol* 2015;46:627–9.
- Gaertner DJ, Hallman TM, Hankenson FC, Batchelder MA. Anesthesia and analgesia for laboratory rodents. In: Fish, R.E., Danneman, P.J., Brown, M., Karas AZ, editor. *Anesthesia and Analgesia in Laboratory Animals*. 2nd ed. Elsevier Academic Press, London (UK); 2008:239–97.
- Gamble M. The Hematoxylins and Eosin. In: Bancroft, JD and Gamble M, editor. *Theory and Practice of Histological Techniques*. 6th ed. Philadelphia: Churchill Livingstone Elsevier; 2008:121–34.
- Buchwalow IB, Böcker W. Working with Antibodies. In: *Immunohistochemistry: Basics and Methods*. Springer Berlin Heidelberg; 2010:31–9.
- Bozzola JJ, Russell LD. Specimen Preparation for Transmission Electron Microscopy. In: *Electron Microscopy: Principles and Techniques for Biologists*. 2nd ed. Sudbury, MA: Jones and Bartlett publishers; 1999:16–47.
- Ibrahim MAA, Elwan WM, Elgendi HA. Role of Scutellarin in Ameliorating Lung Injury in a Rat Model of Bilateral Hind Limb Ischemia-Reperfusion. *Anat Rec* 2019;302:2070–81.

21. Dawson B, Trapp RG. Basic & Clinical Biostatistics. In: Basic & Clinical Biostatistics. 4th ed. Lange Medical Books / McGraw-Hill Medical Publishing Division; 2004:162–89.
22. Santos-Júnior FFU, Pires A de F, Ribeiro NM, et al. Sensorial, structural and functional response of rats subjected to hind limb immobilization. *Life Sci* 2015;137:158–63.
23. Catalá A, Díaz M. Editorial: Impact of Lipid Peroxidation on the Physiology and Pathophysiology of Cell Membranes. *Front Physiol* 2016;7:423.
24. Khalil RM, Abdo WS, Saad A, Khedr EG. Muscle proteolytic system modulation through the effect of taurine on mice bearing muscular atrophy. *Mol Cell Biochem* 2017;444:161–8.
25. Oyenihu AB, Ollewagen T, Myburgh KH, Powrie YSL, Smith C. Redox Status and Muscle Pathology in Rheumatoid Arthritis: Insights from Various Rat Hindlimb Muscles. *Oxid Med Cell Longev* 2019;2019:2484678.
26. Appell HJ, Ascensão A, Natsis K, Michael J, Duarte JA. Signs of Necrosis and Inflammation Do Not Support the Concept of Apoptosis as the Predominant Mechanism During Early Atrophy in Immobilized Muscle. *Basic Appl Myol* 2004;14:191–6.
27. Gomes ARS, Coutinho EL, França CN, Polonio J, Salvini TF. Effect of one stretch a week applied to the immobilized soleus muscle on rat muscle fiber morphology. *Brazilian J Med Biol Res* 2004;37:1473–80.
28. Nascimento CCF, Padula N, Milani JGPO, Shimano AC, Martinez EZ, Mattiello-Sverzut AC. Histomorphometric analysis of the response of rat skeletal muscle to swimming, immobilization and rehabilitation. *Brazilian J Med Biol Res* 2008;41:818–24.
29. Dumitru A, Radu BM, Radu M, Cretoiu SM. Muscle Changes During Atrophy. *Adv Exp Med Biol* 2018;73:92.
30. Bonaldo P, Sandri M. Cellular and molecular mechanisms of muscle atrophy. *Dis Model Mech* 2013;6:25–39.
31. Fichna JP, Karolczak J, Potulska-Chromik A, et al. Two desmin gene mutations associated with myofibrillar myopathies in Polish families. *PLoS One* 2014;9:e115470–e115470.
32. Carraro U, Kern H. Severely Atrophic Human Muscle Fibers With Nuclear Misplacement Survive Many Years of Permanent Denervation. *Eur J Transl Myol* 2016;26:5894.
33. Manhart A, Windner S, Baylies M, Mogilner A. Mechanical positioning of multiple nuclei in muscle cells. *PLoS Comput Biol* 2018;14:e1006208–e1006208.
34. de Oliveira Nunes Teixeira V, Filippin LI, Viacava PR, de Oliveira PG, Xavier RM. Muscle wasting in collagen-induced arthritis and disuse atrophy. *Exp Biol Med* 2013;238:1421–30.
35. Arentson-Lantz EJ, English KL, Paddon-Jones D, Fry CS. Fourteen days of bed rest induces a decline in satellite cell content and robust atrophy of skeletal muscle fibers in middle-aged adults. *J Appl Physiol* 2016;120:965–75.
36. Zhang S-F, Zhang Y, Li B, Chen N. Physical inactivity induces the atrophy of skeletal muscle of rats through activating AMPK/FoxO3 signal pathway. *Eur Rev Med Pharmacol Sci* 2018;22:199–209.
37. Mammucari C, Milan G, Romanello V, et al. FoxO3 Controls Autophagy in Skeletal Muscle In Vivo. *Cell Metab* 2007;6:458–71.
38. Zhao J, Brault JJ, Schild A, et al. FoxO3 Coordinately Activates Protein Degradation by the Autophagic/Lysosomal and Proteasomal Pathways in Atrophying Muscle Cells. *Cell Metab* 2007;6:472–83.
39. Bodine SC, Latres E, Baumhueter S, et al. Identification of Ubiquitin Ligases Required for Skeletal Muscle Atrophy. *Science* 2001;294:1704–8.
40. Gomes MD, Lecker SH, Jagoe RT, Navon A, Goldberg AL. Atrogin-1, a muscle-specific F-box protein highly expressed during muscle atrophy. *Proc Natl Acad Sci U S A* 2001;98:14440–5.
41. Lokireddy S. Loss of Mitochondria during Skeletal Muscle Atrophy. *Autophagy Cancer, Other Pathol Inflammation, Immunity, Infect Aging* 2014;239–51.
42. Huang Z, Fang Q, Ma W, et al. Skeletal Muscle Atrophy Was Alleviated by Salidroside Through Suppressing Oxidative Stress and Inflammation During Denervation. *Front Pharmacol* 2019;10:997.
43. Powers SK, Smuder AJ, Judge AR. Oxidative stress and disuse muscle atrophy: cause or consequence? *Curr Opin Clin Nutr Metab Care* 2012;15:240–5.
44. Londhe P, Guttridge DC. Inflammation induced loss of skeletal muscle. *Bone* 2015;80:131–42.
45. Foresto CS, Paula-Gomes S, Silveira WA, et al. Morphological and molecular aspects of immobilization-induced muscle atrophy in rats at different stages of postnatal development: the role of autophagy. *J Appl Physiol* 2016;121:646–60.

46. Chellini F, Tani A, Zecchi-Orlandini S, Sassoli C. Influence of Platelet-Rich and Platelet-Poor Plasma on Endogenous Mechanisms of Skeletal Muscle Repair/Regeneration. *Int J Mol Sci* 2019;20:683.
47. Dimauro I, Grasso L, Fittipaldi S, *et al.* Platelet-rich plasma and skeletal muscle healing: a molecular analysis of the early phases of the regeneration process in an experimental animal model. *PLoS One* 2014;9:e102993–e102993.
48. Borrione P, Fagnani F, Di Gianfrancesco A, Mancini A, Pigozzi F, Pitsiladis Y. The Role of Platelet-Rich Plasma in Muscle Healing. *Curr Sports Med Rep* 2017;16:459–63.
49. Alves R, Grimalt R. A Review of Platelet-Rich Plasma: History, Biology, Mechanism of Action, and Classification. *Ski appendage Disord* 2018;4:18–24.
50. Borrione P, Fossati C, Pereira MT, *et al.* The use of platelet-rich plasma (PRP) in the treatment of gastrocnemius strains: a retrospective observational study. *Platelets* 2017;29:596–601.
51. Setayesh K, Villarreal A, Gottschalk A, Tokish JM, Choate WS. Treatment of Muscle Injuries with Platelet-Rich Plasma: a Review of the Literature. *Curr Rev Musculoskelet Med* 2018;11:635–42.

الملخص العربي

البلازما الغنية بالصفائح الدموية تعزز تعافي ضمور العضلات الهيكيلية بعد إجهاد التثبيت في الجرذان: دراسة هستولوجية و هستوكيميائية مناعية

هبة حسن القليني، شيرين شوقي العبد، مروة عوض عبد الحميد إبراهيم
قسم الهستولوجيا وبيولوجيا الخلية - كلية الطب - جامعة طنطا

مقدمة: يحدث إجهاد التثبيت في حالات سريرية مختلفة كالأمراض الالتهابية والعصبية العضلية المزمنة مما يؤدي إلى ضمور العضلات الناتج عن عدم الاستخدام. تعافي العضلات الهيكيلية بعد التثبيت بطيء وغير مكتمل. تم استخدام البلازما الغنية بالصفائح الدموية لتحسين إصابات العضلات، ومع ذلك لم يتم دراسة دورها في تسريع شفاء العضلات عند إجهاد التثبيت.

الهدف من العمل: دراسة التأثير المساعد المحتمل للعلاج بالبلازما الغنية بالصفائح الدموية على ضمور العضلات الهيكيلية أثناء التعافي بعد إجهاد التثبيت في الجرذان باستخدام تقنيات هستولوجية و هستوكيميائية مناعية مختلفة.

مواد و طرق البحث: تم تقسيم ستة وثلاثين من ذكور الجرذان البالغة بالتساوي إلى أربع مجموعات. الضابطة، المثبتة (مقيدة في أقفال صغيرة الحجم لمدة 4 أسابيع)، التعافي وحده (4 لمدة أسبوع)، ومجموعات التعافي مع البلازما الغنية بالصفائح الدموية. تمت معالجة عينات العضلات الهيكيلية لدراسات هستولوجية و هستوكيميائية مناعية.

النتائج: أظهرت المجموعة المثبتة انقساماً في الألياف العضلية، واستيعاباً للأئوية، وقداناً لتخيط الألياف، وتمويلًا وقطعًا للساركوميلا و علامات التهاب. كشف الفحص الدقيق عن وجود خلايا عضلية ذات نوى مسننة، ومتوكوندريا ذات شكل وحجم غير طبيعي، وضمور عضلي مع فقدان الخيوط العضلية وانقسام الليفبات العضلية. تم تسجيل انخفاض ذي دلالة احصائية في كل من متوسط مساحة المقطع العرضي للألياف العضلية ومتوسط النسبة المئوية لمساحة الألياف العضلية مع انخفاض كبير في التعبير الهستوكيميائي المناعي لـ desmin. كشفت مجموعة التعافي استمرار التغيرات الهستولوجية و الهيستوكيميائية المناعية. بينما أظهرت مجموعة التعافي و البلازما الغنية بالصفائح الدموية شكلاً شبه طبيعي مع اختلاف غير ذي دلالة احصائية في التعبير الهستوكيميائي المناعي لـ desmin مقارنة بالمجموعة الضابطة.

الاستنتاج: قدمت البلازما الغنية بالصفائح الدموية تحسيناً واعداً لضمور العضلات بعد إجهاد التثبيت. يوصى بتطبيق العلاج بالبلازما الغنية بالصفائح الدموية كعلاج مساعد أثناء التعافي بدلاً من التعافي وحده.